Eur. Phys. J. A (2024) 60:27
https://doi.org/10.1140/epja/s10050-024-01235-4

THE EUROPEAN PHYSICAL JOURNAL A

Regular Article - Theoretical Physics

# Detailed modeling of odd–even staggering in fission-fragment charge distributions

## Damping of staggering effects with excitation energy and compound-nucleus charge

**Peter Möller**[1,a], **Christelle Schmitt**[2]

[1] Mathematical Physics, Lund University, 221 00 Lund, Sweden
[2] Institut Pluridisciplinaire Hubert Curien (IPHC), Rue du Loess, 67000 Strasbourg, France

Received: 26 September 2023 / Accepted: 3 January 2024 / Published online: 7 February 2024

Communicated by Cedric Simenel

**Abstract** During the last 10 years or so the Brownian shape-motion (BSM) model has been used in numerous calculations of fission-fragment mass and charge distributions with encouraging agreement with experimental measurements. In this model the structure obtained in the fission-fragment distributions is entirely a consequence of the structures in the calculated five-dimensional (5D) potential-energy surfaces. The potential-energy model until recently did not accommodate the influence of the emerging fragment properties on the calculated potential energy. Therefore there were no odd-even effects in the calculated fission-fragment distributions. Recent extensions of the potential-energy model allow properties of the nascent fragments to be included in the potential-energy model. Application of the BSM model to execute random walks on these more detailed potential-energy surfaces led to calculated fission-fragment yields that exhibited odd-even effects, which "by eye" indicated reasonable agreement with experimental data. The present work goes a step further with a quantitative comparison between experimental and theoretical results based on the global and local odd-even staggering observables. Theoretical calculations and experimental observations both show that pairing effects and enhancement of two-nucleon relative to one-nucleon transfer in heavy-ion collisions decrease with excitation energy and implementing a damping of these quantities with excitation energy leads to improved agreement with experiment. Characteristic variations of the local staggering with charge split seen in the experimental data are also present in the calculated results.

## 1 Introduction

In the Brownian shape-motion (BSM) method fission-fragment yields are calculated by random walks on a five-dimensional (5D) potential-energy "surface" which is a function of five shape variables. The 5D potential-energy function is calculated for a discrete set of about five million different shapes and stored as a 5D matrix, see Ref. [1] for more details. The BSM method was introduced in 2011 [2]. Subsequently it has been extensively tested with respect to experimental data. A phenomenological treatment of the damping of the shell corrections with energy was introduced at the time of these tests [3]. In the study of Ref. [3] the calculated fragment charge yields compared well with the 70 yield distributions measured at GSI [4]. In Ref. [5] the sensitivity of the method to various model ingredients was investigated, in particular to the discretization of the shape space and to various assumptions about the dissipation tensor [3]. The charge yield was found to be relatively robust with respect to these aspects, so an explicit dissipation tensor is not implemented in the current model, although an implicit assumption underlying the BSM model is strong dissipation. However, a potential-energy surface of lower dimensionality is unable to describe the experimental data, demonstrating the importance of the choice and number of collective coordinates. After these studies and benchmarks had been carried out the model was used to calculate fission yields for 987 nuclides [6] so that its predictive capabilities can be tested in future experiments.

[a] e-mail: mollerinla@gmail.com (corresponding author)

## 2 Calculational details

The potential energies are calculated as specified in detail in Ref. [1]. All total potential energies in this work (in tables, figures, and text) are expressed with respect to our defined reference point, the macroscopic energy of the spherical shape for the particular nuclide considered. The selected shape grid-points in the shape variables $Q_2$ (elongation), $r_n$ (neck radius), $\epsilon_{f1}$ (left fragment deformation), and $\epsilon_{f2}$ (right fragment deformation) are as in Ref. [1]. The asymmetry variable $\alpha_g$ is chosen so that each value of this coordinate corresponds to integer values of $Z_1$ and $Z_2$ in the fragments. The model enhancements introduced to study odd-even staggering are presented in Ref. [7]. Each fragment distribution calculation is based on 500,000 trajectories or random walks. The walks are started in the ground state and terminated when the neck radius is 2.5 fm. The bias-potential constant $V_0$ is 15 MeV [2].

### 2.1 Nascent fragment pairing effects

We summarize how we previously modeled odd–even effects. When the fragments are fully developed with zero neck radius of the compound system a common assumption is that for odd–odd splits the extra odd contribution to the energy should be $E_{odd} = 2\times\Delta$ where $\Delta$ is the pairing-gap parameter, which we in previous work [8] have chosen as $\Delta = 1.0$ MeV. With a non-zero neck radius the effect of pairing of the emerging odd splits would be smaller; for very compact shapes with no obvious neck there should be no effect. This leads to the following prescription for the odd energy contribution to the fissioning system

$$\begin{aligned} E_{odd} &= 2\times\Delta\times(B_W-1)^k \quad \text{odd} \quad Z_1, Z_2 \\ E_{odd} &= 0 \qquad\qquad\qquad\quad \text{even} \quad Z_1, Z_2 \end{aligned} \tag{1}$$

where, with the choice $k = 1$, $(B_W - 1)^k$ has been our choice [7,9] for the shape-dependence ansatz for the Wigner term in our potential-energy model. The shape factor $B_W$ is 1 for a shapes with no neck and increases continuously, as the neck develops, to 2 for separated fragments. It is necessary to postulate such a shape dependence because the macroscopic energy of two separated fragments contains two Wigner terms, the original system only one. Without such a shape dependence a discontinuity of the order of 10 MeV would occur at scission of actinide nuclei. That is, if we calculated the energy for a deforming nucleus up to the scission point we would at scission obtain a 10 MeV lower energy than if we calculated the energy of two approaching separated fragments. A pedagogical figure illustrating this and the necessity of this shape dependence is in Ref. [10], fig. 1. Since we need a realistic potential-energy surface in the scission region we do need to consider these issues, which have in many investigations been ignored. The comprehensive discussion of the shape-dependence of the Wigner term in Ref. [9] carries directly over to how the effect of the pairing $\Delta$ increases as the neck becomes narrower. There is no known derivation of the shape dependence of the Wigner term, so it was postulated, based on consideration of its behavior in the limit of fully developed fragments [9]. The power constant $k$, governs how early in the division process the character of the two fragments causes the "second" Wigner term, and additionally in our case, the odd pairing effect, start to appear.

In addition to allowing pairing effects in the nascent fragments to modify the model of the potential energy when the fragments start to exhibit their individual characters, the random walk also needs to be further developed. In its initial formulation a candidate point for the next step in the random walk is a point adjacent to the current point [2]. However, when there is a large difference in yield for even-even splits compared to odd-odd splits, high for the former and low for the latter, the random walk has to traverse a low-yield "choke point" to reach the next high-yield point on the fragment charge-distribution curve. This "choke point" would greatly reduce the probability of populating the next even-even point on the charge-yield curve. So might two protons be transmitted in one step? This possibility was implemented in our first study of odd-even staggering [7], namely we selected as a possible next candidate point in the asymmetry direction in the random walk a point corresponding to a change by one proton and a change of two protons with equal probability. There is experimental evidence of enhanced probability in heavy-ion collisions of transferring two nucleons in one step compared to a two-step process, see Ref. [11] and references cited in Ref. [7]. In the latter it was pointed out that both the magnitude of the pairing $\Delta$ added to the potential energy and the relative probabilities of selecting one step or two step candidate points in the charge-asymmetry variable would need to depend on excitation energy in a more refined formulation. In our work "transfer" refers to moving nucleons from one emerging fragment to the other, that is changing the asymmetry coordinate in the calculated potential-energy surface. Now new detailed experimental studies of staggering in fission-fragment charge distributions have become available for several fissioning nuclei and excitation energies, see Ref. [12] and references therein. Therefore we are now in a position to compare calculated and experimental global and local staggering quantities and their variation with excitation energy, element and isotope.

### 2.2 Adaptation of the Brownian shape-motion random-walk to charge-yield modeling

In our investigations here the charge yield is calculated with the original "five-dimensional" $Y(A)$ code [2,5] by varying the volume asymmetry $(A_1, A_2)$ where the compound

nucleon number $A$ is $A = A_1 + A_2$ so that these volume splits yield fragment $(Z_1, Z_2)$ splits that are integers, with the assumption of unchanged charge division (UCD).

The charge yields in Ref. [7] are calculated by use of that approach. Calculated yields without and with pairing effects in the emerging fragments are shown in the top and bottom panels of fig. 1, in this initial model no damping of pairing effects with energy were included. In other studies, such as modeling isotopic yields [13] it is necessary to use the full "six-dimensional" model that allows calculation of $Y(Z, N)$ which was also introduced in Ref. [7]. In our previous studies of staggering effects in fission-fragment charge distributions comparisons between experimental and theoretical results were simply done by overlaying the experimental and theoretical charge distributions in the same figures, see for example [7,13,14].

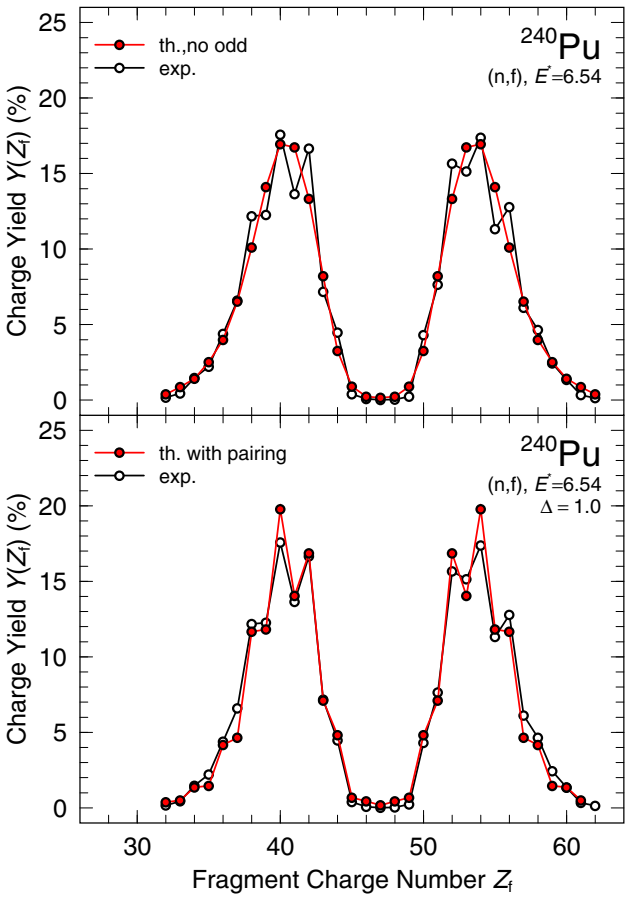


**Fig. 1** Calculated and experimental fission-fragment charge distributions for $^{240}$Pu. Fragment pairing effects are not included in the top panel but are in the bottom panel. The units of $E^*$ and $\Delta$ are MeV

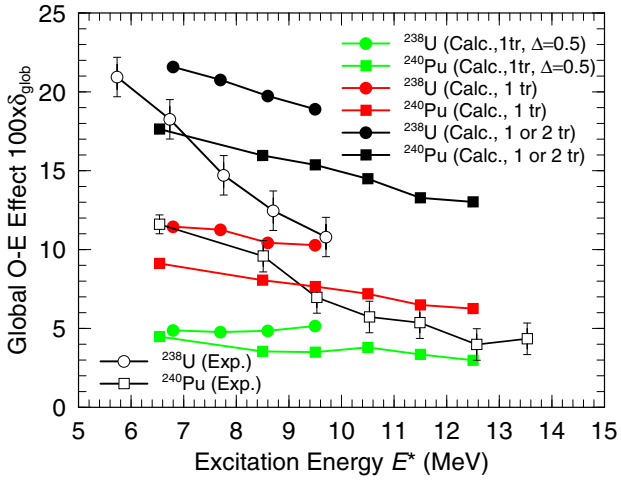


**Fig. 2** Experimental studies of how $\delta_{glob}$ depends on excitation energy for two compound systems (Open symbols). The filled black symbols (upper group of symbols) are the calculated results with our model as defined in Ref. [7]. The red filled (middle) group of calculated symbols are the results when we only allow the next neighbor as a candidate next point in the random walk. Finally the green (lower) group of calculated results are obtained when we *also* decrease the pairing delta to $\Delta = 0.5$ MeV

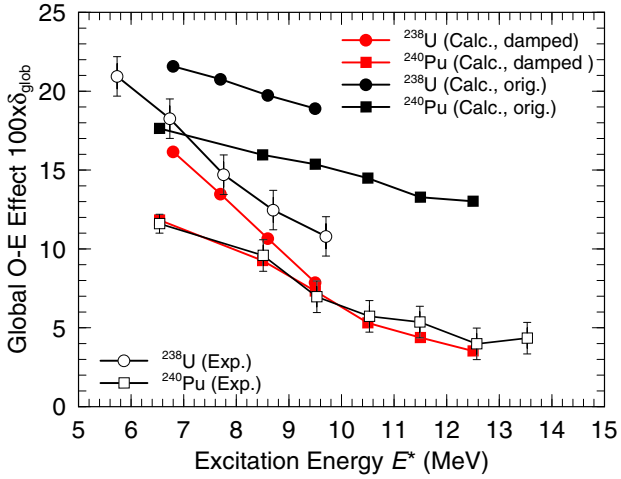


**Fig. 3** Variation of calculated $\delta_{glob}$ with excitation energy and element, with our selected damping of $\Delta_{pair}$ and selected damping of paired proton transfers, red filled symbols (lower group of filled symbols). Experimental results are shown as open symbols. Results with original model [7] (no damping of pairing or two proton transfer with energy) are shown as filled black symbols (upper group of filled symbols). Only one calculated point is significantly outside the experimental error bars

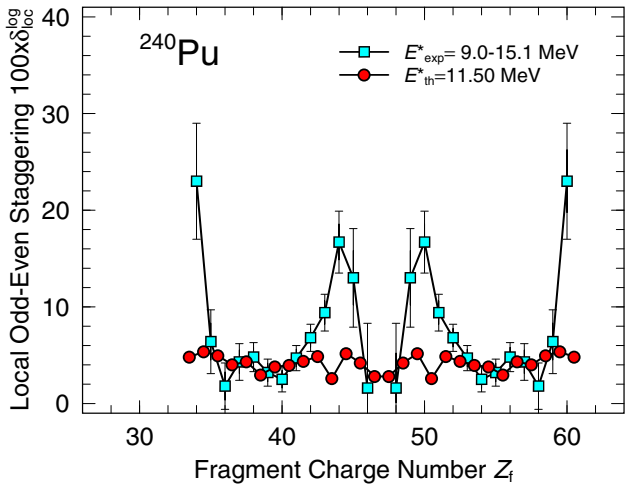


**Fig. 4** Local staggering $\delta_{\text{loc}}^{\log}$ from experiment [16] at an average energy of 11.5 MeV compared to calculations based on our current model

### 2.3 Global staggering in fission-fragment charge distributions

In Ref. [15] a global measure $\delta_{\text{glob}}$ of odd-even staggering in nuclear charge yields is defined as

$$\delta_{\text{glob}} = \frac{1}{\sum_Z Y(Z)} \sum_Z (-1)^Z Y(Z) \tag{2}$$

We show in fig. 2 measured $\delta_{\text{glob}}$ for $^{238}$U and $^{240}$Pu for a range of excitation energies [16]. As expected [17] the measured value of $\delta_{\text{glob}}$ decreases with increasing excitation energy and with increasing charge of the fissioning compound nuclide. The same is true for the $\delta_{\text{glob}}$ calculated in our original model [7], but the calculated values do not decrease sufficiently fast versus energy or compound system. A comprehensive review of experimental results are in [18,19].

### 2.4 Damping of fission-fragment pairing effects with excitation energy

First, let us alert to the two uses of "excitation energy". In experiments excitation energy usually means excitation energy (above the ground state) of the compound nucleus. In our theory discussions in most contexts we mean the excitation on the random walk trajectory above the current point in the potential energy surface, which is a function of the current shape and the initial energy imparted to the nucleus. The meaning should be clear from context.

Pairing studies [20,21] show that the pairing gap $\Delta$ and other pairing effects decrease with energy. We can therefore anticipate that also the probability of transferring paired protons in one step decreases with excitation energy. In Fig. 2 we have studied the effect on $\delta_{\text{glob}}$ of not allowing transfer of two protons in one step, shown as filled red symbols (middle group of calculated results) and in the lower green group the effect of a smaller pairing delta, namely $\Delta = 0.5$ MeV, *and* not allowing transfer of two paired protons in one step. Because experimental results and calculations (see for example figures in [20]) show little decrease of the pairing $\Delta$ for low excitation energies we have in our model (and codes) implemented

$$\begin{aligned} \Delta &= e^{(-0.17\times(E^*-6))} \times 1.0 \quad E^* \geq 6.0 \ \text{MeV} \\ \Delta &= 1.0 \ \text{MeV} \qquad\qquad\quad E^* \leq 6.0 \ \text{MeV} \end{aligned} \tag{3}$$

Specifically, fig. 3 in Ref. [20] shows almost no decrease in $\Delta$ for low excitation energies after which there is a rapid decrease; the above expression was formulated to approximate this behavior and the constants adjusted to reproduce the observed values of the global pairing quantity $\delta_{\text{glob}}$ defined in Eq. 2. In our original model of odd-even fission-fragment charge-distribution staggering we picked one or two steps in the asymmetry variable (integer proton number) as the next candidate point on the random walk trajectory with equal probability. Recognizing that the probability of transferring two paired protons together in one step decreases with excitation energy leads us to the following modified selection algorithm. First a candidate point for one or two steps in the asymmetry coordinate is selected as before with equal probabilities. If the outcome is that two steps are suggested for a candidate point, then to decrease the probability of going two steps in the asymmetry coordinate when the excitation energy increases, we add the following step. We execute the random number generator (in the range 0 to 1) again. If it is larger than $0.6 * e^{(-0.07*E^*)}$ we do not use the candidate point obtained but start the process over. This decreases the probability that a candidate point corresponding to transfer of two protons is selected as the energy increases.

In Fig. 3 we compare $\delta_{\text{glob}}$, calculated with damping according to the above discussion included, to available experimental data. Only one of the calculated points is significantly outside the experimental error bars for the ten data points studied.

### 2.5 Local staggering in fission-fragment charge distributions

Tracy et al. [22] define a local odd-even staggering measure $\delta_{\text{loc}}$ which specifically applied to charge yields [15] is written

$$\begin{aligned} \delta_{\text{loc}}^{\log}\left(Z+\frac{3}{2}\right) = \frac{(-1)^Z}{8}\Big[&\ln Y(Z+3) - \ln Y(Z) \\ &-3\Big(\ln Y(Z+2) - \ln Y(Z+1)\Big)\Big] \end{aligned} \tag{4}$$

One should note that this is a "logarithmic" definition. The consequence is that (in a figure) a 0.1% deviation where the

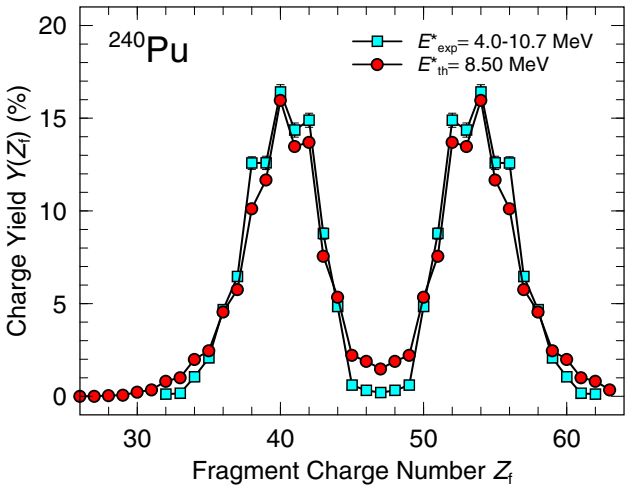


**Fig. 5** Measured fission-fragment charge yields [16], at an average energy 8.5 MeV, compared to calculated values

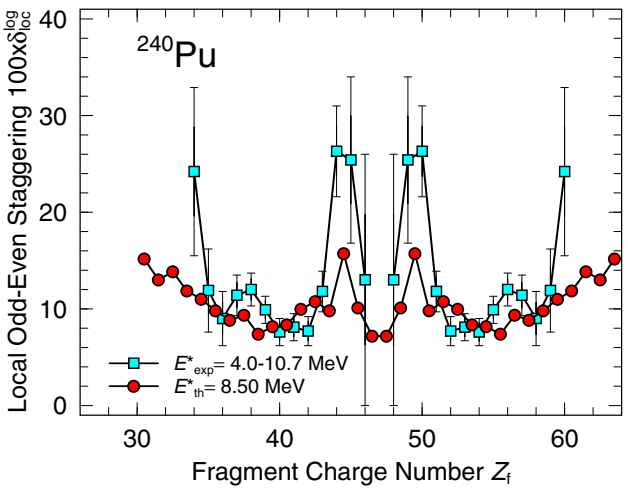


**Fig. 6** Local staggering $\delta^{\log}_{\rm loc}$ from experiment [16], compared to values calculated in our current study. With this logarithmic definition of $\delta^{\log}_{\rm loc}$, deviations appear large in regions of low yield, as they also will in similar figures below

yield is 1% will look as large as a 1% deviation where the deviation is 10%. As a consequence small yield deviations in low-yield regions will look large. However, in practical applications one might be more interested in the deviations where the yield is high, where the effect on some studied process would affect the outcome the most. Then the "non-logarithmic" expression

$$\delta^{\rm lin}_{\rm loc}\left(Z+\frac{3}{2}\right)=\frac{1}{\sum_Z Y(Z)}\left\{\frac{(-1)^Z}{8}\Big[Y(Z+3)-Y(Z) -3\Big(Y(Z+2)-Y(Z+1)\Big)\Big]\right\} \quad (5)$$

would be the most appropriate. Also, if we assume the inaccuracy of the calculations is more "absolute" than relative and that one (of unknown source) contribution to the theoretical error in the yield is, say, 1% for any mass split, then it would be difficult to get small logarithmic errors in the local staggering $\delta^{\log}_{\rm loc}$ in the tails of the charge distributions and also in the symmetry region where the yield for the cases we study is also low. We will below compare the logarithmic and linear measures of looking at local odd-even staggering.

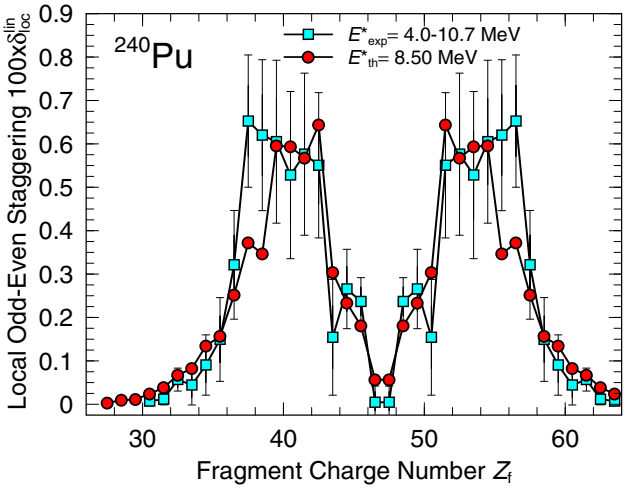


**Fig. 7** Local staggering $\delta^{\rm lin}_{\rm loc}$ from experiment [16] compared to calculated values for compound-nucleus excitation energy 8.50 MeV. Here the use of a linear version of $\delta_{\rm loc}$ leads to the impression that the largest differences occur in the high-yield regions

## 3 Results and discussion

We compare calculated local staggering to recent experimental results [16] for a range of energies for fission of $^{240}$Pu and $^{238}$U. For $^{240}$Pu the comparisons are in Figs. 4, 5, 6, 7, and 8. At the compound-nucleus excitation energy 8.5 MeV in Figs. 5, 6, and 7 we study three quantities, namely the fission-fragment charge distribution, the local logarithmic staggering $\delta^{\log}_{\rm loc}$ and the local linear staggering $\delta^{\rm lin}_{\rm loc}$ to show these three related quantities for one specific energy. For $^{238}$U we study the local logarithmic staggering $\delta^{\log}_{\rm loc}$ for the two compound-nucleus excitation energies 8.7 MeV and 6.8 MeV in Figs. 9 and 10. The charge yield for $^{240}$Pu at 8.5 MeV shows that the rather small deviation in the yield at $Z = 38$ gives a substantial deviation in the linear local odd–even staggering $\delta^{\rm lin}_{\rm loc}$ at $Z = 38$ and $Z = 39$ The deviation at, for example, $Z = 34$ appears small whereas in the logarithmic plot it appears large. The deviations at $Z = 38$ and $Z = 39$ in the linear plot in Fig. 7, are about a factor 2 as displayed, whereas in the log plot in Fig. 6 the difference between theory and experiment appears quite small; experiment is about 12 and the calculation is about 10. We should also note that the difference definitions of the local staggering for a specific

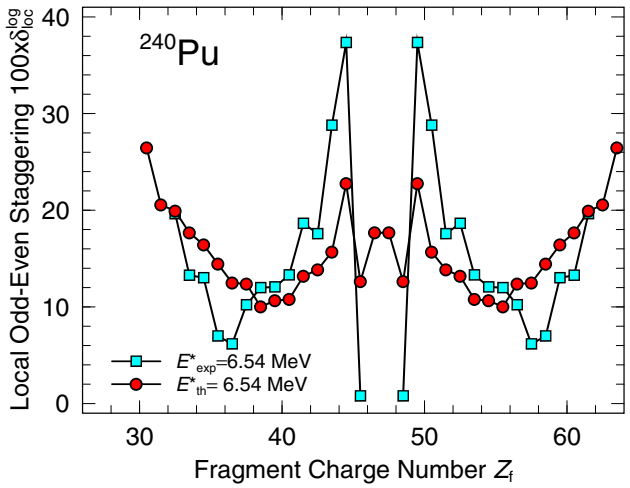


**Fig. 8** Local staggering $\delta^{\log}_{\rm loc}$ obtained from an evaluated experimental data base [23] and calculated from our current study. The heavy-yield peak in the experimental data has been obtained by mirroring the yields in the light peak. The data is for thermal-neutron induced fission

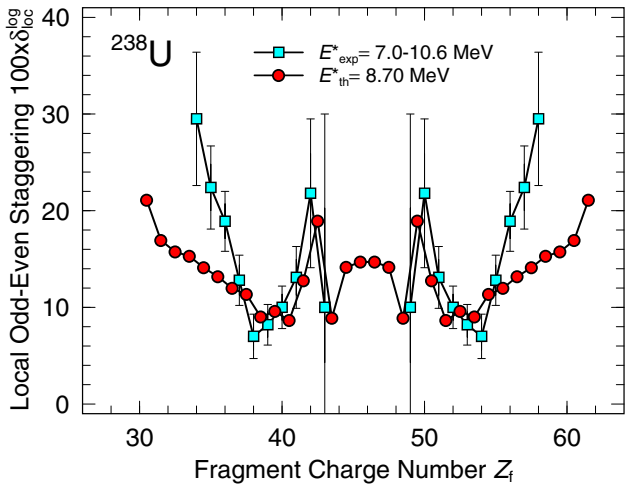


**Fig. 9** Local staggering $\delta^{\log}_{\rm loc}$ from experiment [16] compared to calculations for an average experimental compound-nucleus excitation energy of 8.70 MeV

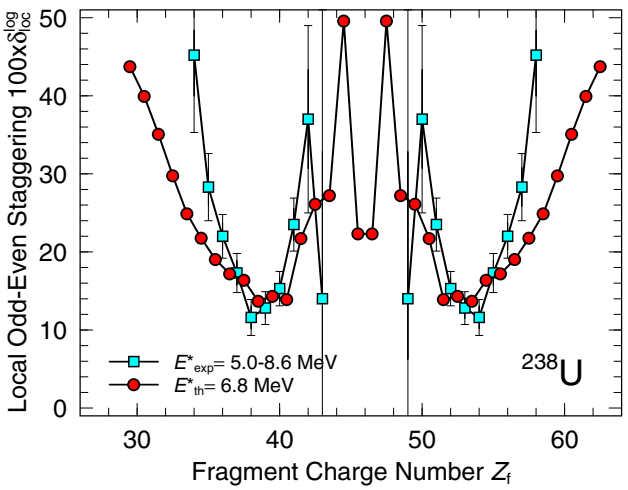


**Fig. 10** Local staggering $\delta^{\log}_{\rm loc}$ from experiment [16] compared to calculations for an average experimental compound-nucleus excitation energy of 6.80 MeV

proton number have contributions from the actual mass yield at four different proton numbers.

One needs to be aware that difference expressions like the ones used here to extract some quantity from experimental data have limitations in many situations. It is well-known that pairing effects, in particular an "experimental" value of the pairing gap $\Delta$, are often extracted from experimental masses by difference expressions, see for example Refs. [24,25]. However, in the specific example of pairing these difference expressions extract all non-smooth contributions to the mass surface beyond second order, from for example, and very importantly, contributions from deformation changes. However, if experimental and theoretical "pairing gaps" are based on using the same difference expressions on experimental and theoretical masses they can be compared, although they do not exactly correspond to pairing gaps used or obtained in theoretical models. The same is of course correct for the local staggering measures. But as pointed out above we need to be aware of how differently linear and logarithmic deviations present the experimental data. We can still draw some general conclusions and we find encouraging agreement between experimental and theoretical results. In particular, a general feature in the experimental results is that local staggering increases toward the tails of the yields, towards symmetric divisions, and decreases with excitation energy. These features are also seen in the theoretical results. In the logarithmic local staggering calculations the larger deviations with respect to experiment occur in the regions of low yield, which we explained above occur because the logarithmic definition will give large deviations in regions of low yield even if the deviation is only a fraction of a percent.

In Fig. 8 there is an obvious large deviation at $Z = 36$ and $Z = 35$ which occurs because there is a large bump in the experimental data. In this case the experimental data is from an ENDEF *evaluation* [23]. The evaluation lists the isotopic yields $Y(Z, N)$ for which we have taken the obvious sums to obtain $Y(Z)$. Additionally, we have obtained the heavy peak by reflecting on symmetric division. There is no similar bump in the newly measured data [16] at closelying excitation energies for these proton numbers, see for example Fig. 5. It therefore seems clear that additional experimental measurements are needed for thermal-neutron-induced fission for $^{240}$Pu so that more accurate yields will be available.

At higher excitation energies, the experimental data correspond to a range of excitation energies, see legends in Figs. 4, 5, 6, 7, 9, 10, rather than to a well-defined value. The calculations were instead performed for a specific value, chosen

approximately as the mean of the energy range, due to the imprecise knowledge of the excitation-energy distribution in the experiments. Furthermore, due to low statistics, the experimental error bars can be quite large, as is seen in the figures. A more refined study of the rate of damping of staggering effects requires more precise experimental information. Measurements in this direction are currently in progress [26].

It is common in many contexts to use a phenomenological expression for the damping of shell corrections with excitation energy. Such phenomenological damping is also used in the BSM model [3]. It was also shown that use of a Fermi-gas level-density model [27] gave almost identical results compared to a microscopic combinatorial level-density model. However, to model staggering which is due to pairing effects in the emerging fragments it is necessary to introduce in the potential-energy model such pairing effects, as discussed above. Also in this case we have here found that a phenomenological ansatz for the damping with energy of pairing effects is sufficient to yield realistic results. Thus, in the BSM model the structure in the calculated mass and charge yields is determined by the structure in the calculated potential-energy surfaces with the generalization to include effects of pairing properties of the emerging fragments. It is important to note that near scission the potential energy is close to the sum of the fragment ground-state masses plus the Coulomb interaction energy which latter is trivial. This is illustrated in fig. 1 in Ref. [10]. Therefore it is important that the potential-energy model yields sufficiently accurate ground-state masses. In the potential-energy model used here the ground-state masses are accurate to about 0.75 MeV [10].

However to describe neutron emission from the fission fragments and correlations between fragment total kinetic energies, mass division and number of neutrons emitted it is necessary to calculate microscopic level structure in the emerging fragments [28].

**Acknowledgements** This work was made possible by an invitation to PM from GANIL for a two-month visit in the fall of 2022, which is gratefully acknowledged. We have also benefited from discussions with M. Caamaño, A. Lemasson, D. Ramos, H. Sagawa, and Yi-Fei.

**Funding** Open access funding provided by Lund University.

**Data Availability Statement** This manuscript has no associated data or the data will not be deposited. [Authors' comment: This is a theory paper, no data collected. Experimental data used are in cited references.]



## References

1. P. Möller, A.J. Sierk, T. Ichikawa, A. Iwamoto, R. Bengtsson, H. Uhrenholt, S. Åberg, Phys. Rev. C **79**, 064304 (2009)
2. J. Randrup, P. Möller, Phys. Rev. Lett. **106**, 132503 (2011)
3. J. Randrup, P. Möller, Phys. Rev. C **88**, 064606 (2013)
4. K.-H. Schmidt, S. Steinhäuser, C. Böckstiegel, A. Grewe, A. Heinz, A.R. Junghans, J. Benlliure, H.-G. Clerc, M. de Jong, J. Müller, M. Pfützner, B. Voss, Nucl. Phys. A **665**, 221 (2000)
5. J. Randrup, P. Möller, A.J. Sierk, Phys. Rev. C **84**, 034613 (2011)
6. P. Möller, J. Randrup, Phys. Rev. C **91**, 044316 (2015)
7. P. Möller, T. Ichikawa, Eur. Phys. J. A **51**, 173 (2015)
8. P. Möller, A.J. Sierk, T. Ichikawa, A. Iwamoto, M. Mumpower, Phys. Rev. C **91**, 024310 (2015)
9. P. Möller, J.R. Nix, W.J. Swiatecki, Nucl. Phys. A **492**, 349 (1989)
10. P. Möller, A.J. Sierk, A. Iwamoto, Phys. Rev. Lett. **92**, 072501 (2004)
11. L. Corradi, S. Szilner,, G. Pollarolo, G. Colò, P. Mason, E. Farnea, E. Fioretto, A. Gadea, F. Haas, D. Jelavič-Malenica, N. Mărginean, C. Michelagnoli, G. Montagnoli, D. Montanari, F. Scarlassara, N. Soić, A. M. Stefanini, C. A. Ur, and J. J. Valiente-Dobón, Phys. Rev. C **84**, 034306 (2011)
12. D. Ramos, M. Caamaño, F. Farget, C. Rodríguez-Tajes, L. Audouin, J. Benlliure, E. Casarejos, E. Clement, D. Cortina, O. Delaune, X. Derkx, A. Dijon, D. Doré, B. Fernández-Domínguez, G. de France, A. Heinz, B. Jacquot, C. Paradela, M. Rejmund, T. Roger, M.-D. Salsac, C. Schmitt, Phys. Rev. C **99**, 024615 (2019)
13. C. Schmitt and P. Möller Phys. Lett. B **812**, 136017 (2021)
14. P. Möller, C. Schmitt, Eur. Phys. J. A **53**, 7 (2017)
15. D. Ramos, C. Rodríguez-Tajes, M. Caamaño, F. Farget, L. Audouin, J. Benlliure, E. Casarejos, E. Clement, D. Cortina, O. Delaune, X. Derkx, A. Dijon, D. Doré, B. Fernández-Domínguez, G. de France, A. Heinz, B. Jacquot, A. Navin, C. Paradela, M. Rejmund, T. Roger, M.-D. Salsac, C. Schmitt, EPJ Web of Conferences **146**, 04019 (2017)
16. D. Ramos, M. Caamaño, F. Farget, C. Rodríguez-Tajes, A. Lemasson, C. Schmitt L. Audouin, J. Benlliure, E. Casarejos, E. Clement, D. Cortina, O. Delaune, X. Derkx, A. Dijon, D. Doré, B. Fernández-Domínguez, G. de France, A. Heinz, B. Jacquot, C. Paradela, M. Rejmund, T. Roger, M.-D. Salsac, Phys. Rev. C **107**, L021601 (2023)
17. P. Möller, J. Randrup, A. Iwamoto, T. Ichikawa, Phys. Rev. C **90**, 014601 (2014)
18. F. Goennenwein, The Nuclear Fission Process ed. C. Wagemans (London: CRC Press 1991)
19. M. Caamaño, F. Rejmund, K.-H. Schmidt, J. Phys. G: Nucl. Part. Phys. **38**, 035101 (2011)
20. Y.F. Niu, Z.M. Niu, N. Paar, D. Vretenar, G.H. Wang, J.S. Bai, J. Meng, Phys. Rev. C **88**, 034308 (2013)
21. H. Uhrenholt, S. Åberg, A. Dobrowolski, T. Døssing, T. Ichikawa, P. Möller, Nucl. Phys. A **913**, 127 (2013)
22. B. L. Tracy, J. Chaumont, R. Klapisch, J. M. Nitschke, A. M. Poskanzer, E. Roeckl, and C. Thibault, Phys. Rev. C **5** (1972)
23. M.B. Chadwick, P. Obložinský, M. Herman, N.M. Greene, R.D. McKnight, D.L. Smith, P.G. Young, R.E. MacFarlane, G.M. Hale, R.C. Haight, S. Frankle, A.C. Kahler, T. Kawano, R.C. Little, D.G. Madland, P. Möller, R. Mosteller, P. Page, P. Talou, H. Trellue, M. White, W.B. Wilson, R. Arcilla, C.L. Dunford, S.F. Mughabghab, B. Pritychenko, D. Rochman, A.A. Sonzogni, C. Lubitz, T.H. Trumbull, J. Weinman, D. Brown, D.E. Cullen, D. Heinrichs, D.

McNabb, H. Derrien, M. Dunn, N.M. Larson, L.C. Leal, A.D. Carlson, R.C. Block, B. Briggs, E. Cheng, H. Huria, K. Kozier, A. Courcelle, V. Pronyaev, S.C. van der Marck (CSEWG Collaboration), Nuclear Data Sheets, **107**, 2931 (2006)
24. D.G. Madland, J.R. Nix, Nucl. Phys. A **476**, 1 (1988)
25. P. Möller, J.R. Nix, Nucl. Phys. A **536**, 20 (1992)
26. D. Ramos, private communication (2023)
27. D.E. Ward, B.G. Carlsson, T. Døssing, P. Möller, J. Randrup, S. Åberg, Phys. Rev. C **95**, 024618 (2017)
28. M. Albertsson, B.G. Carlsson, T. Døssing, P. Möller, J. Randrup, S. Åberg, Phys. Rev. C **103**, 014609 (2021)